SACLANTCEN MEMORANDUM
serial no.: SM-289

SACLANT UNDERSEA
RESEARCH CENTRE

MEMORANDUM

Statistical characteristics of large-scale bottom reverberation

G. Haralabus

July 1995

Page count for SM-289 (excluding Covers and Data Sheet)

Pages	Total
i–vi	6
1–29	29
	35

SACLANT Undersea Research Centre
Viale San Bartolomeo 400
19138 San Bartolomeo (SP), Italy

tel: +39-187-540.111
fax: +39-187-524.600

e-mail: library@saclantc.nato.int

NORTH ATLANTIC TREATY ORGANIZATION

SACLANTCEN SM-289

Statistical characteristics of large-scale bottom reverberation

G. Haralabus

The content of this document pertains to work performed under Project 02 of the SACLANTCEN Programme of Work. The document has been approved for release by The Director, SACLANTCEN.

Issued by:
Systems Research Division

R. Weatherburn
Division Chief

intentionally blank page

Statistical characteristics of large-scale bottom reverberation

G. Haralabus

Executive Summary: It is well known that reverberation is a limiting factor in most target detection problems. The understanding of reverberation characteristics is particularly useful in the analysis of the received signals used in typical antisubmarine warfare or mine countermeasures scenarios.

This memorandum focuses on the statistical characteristics of large-scale bottom reverberation by means of a propagation model appropriate for a heavily range-dependent environment. The simulation environment used here incorporates a new sound transmission software package based on the parabolic equation method. The ultimate goal is to establish a relationship between seafloor types which possess certain morphological characteristics and reverberation statistics.

It is shown that the variance of reverberation increases proportionally to the bottom height while variations in seafloor correlation length are related to higher-order statistics, namely, the coefficient of excess (or kurtosis).

An approach is presented for the complex problem of modeling and studying large-scale reverberation from a rough, non-deterministic seafloor. To pursue further research in this direction, one must consider additional aspects related to this problem, such as power spectrum analysis, optimization of receiver location, and comparison between theoretical and experimental results.

intentionally blank page

Statistical characteristics of large-scale bottom reverberation

G. Haralabus

Abstract: Simulation results from a statistical characterization of large-scale bottom reverberation from broadband signals are presented. The seafloor profile is parametrized via the surface root-mean-square height and correlation length. A connection between these two parameters and the statistical moments of the backscattered signal is established. It is shown that the variance of reverberation increases proportionally to the seafloor root-mean-square height. On the contrary, the kurtosis (or coefficient of excess) of reverberation appears to be independent of changes in roughness height and related to the terrain's smoothness. In particular, it is shown that kurtosis variations are proportional to changes in the seafloor correlation length.

Keywords: bottom reverberation ∘ parabolic equation ∘ scattering

Contents

1. Introduction 1
2. Statistical analysis of bottom reverberation 3
2.1. Theoretical background 3
2.2. Random surface generation 4
2.3. Scenarios under investigation 5
2.4. Statistical measurements 6
3. Conclusions and future plans 17

References 18

Annex A – Wave propagation models: The parabolic equation model . . . 19
Annex B – The 2WAYPE simulation model 23
Annex C – Random surface generation 29

Acknowledgements: I would like to thank D. Gingras and I. Kirsteins for their continuing guidance throughout this project. I, also, would like to thank A. Bassias, A. Maguer and S. Bongi for their assistance in various aspects of my work. Special thanks to F.B. Jensen and H.G. Schneider for many fruitful discussions which provided a great deal of insight about many topics in underwater acoustics.

1 Introduction

Acoustic reverberation is commonly modeled as a Gaussian stochastic process. However, real data often deviate from this model and demonstrate non-Gaussian statistical behavior [1–3]. In these cases, the characteristics of reverberation are better described using a broader family of probability density functions which are reduced to normal functions when certain conditions are fulfilled [4,5]. The main parameters that control the deviation of reverberation from the nominal Gaussian model are the variance and the coefficient of excess (or kurtosis). In this memorandum, the concentration is on the idea of utilizing these two parameters to predict general morphological features of the ocean floor.

The generation of the simulated seafloor is based on an inverse spectrum method [6]. The bottom roughness is designed to follow Gaussian statistics and its spectrum is controlled by the surface root-mean-square (rms) height and correlation length. The former parameter specifies the size of bottom discontinuities and the latter is a measurement of the terrain smoothness.

This work exploits simulation results from various propagation scenarios to unveil a relationship between the bottom average height and correlation length with moments of the backscattered signal time series. Therefore computer simulation programs designed for heavily range-dependent propagation channels are of paramount importance. For this reason the 2WAYPE [7–9] program is chosen for the generation of the synthetic reverberation data. 2WAYPE solves the sound propagation problem using the parabolic equation method.

The goal of this project is not to find an analytical connection between the morphology of the random seafloor and the statistical signature of reverberation. This is an initial attempt to remotely extract bottom features from reverberation signals in a qualitative way. Therefore the analysis is limited to a statistical framework which does not incorporate information about the physics involved in the interaction of the transmitted sound waves with the boundaries.

Section 2 provides the theoretical background for the statistical analysis of reverberation, followed by a description of the random surface generation algorithm. Then, simulation scenarios with the corresponding measurements are presented. Comparisons are made between various cases and certain trends followed by the estimated parameters are observed. A short discussion explains why signals created from different families of random profiles demonstrate particular statistical behavior.

Section 3 presents conclusions and future plans.

Annex A is an overview of the three main methods for solving sound propagation problems, namely, the normal mode, ray tracing, and parabolic equation method. A comparison between the three techniques summarizes the advantages and disadvantages of each one. Special emphasis has been placed on the mathematical background of the PE method, together with the assumptions and the approximations necessary for the implementation of this model.

Annex B presents a few examples of the 2WAYPE program. Results from this program are compared with the outcome of the COUPLE program [10,11]. The sensitivity of 2WAYPE to large-scale (compared to the transmitted wavelength) bottom features is demonstrated.

Annex C lists the MATLAB code used for the generation of the random surface.

2

Statistical analysis of bottom reverberation

2.1. THEORETICAL BACKGROUND

The reverberation signal represents a summation of a random number of elementary scattered signals arriving simultaneously at the point of reception and having random amplitudes and phases. It is usually modeled as a quasi-harmonic function which can be written in the following form:

$$R(t) = A(t)e^{i(\omega_0 t+\varphi(t))}, \tag{1}$$

where $A(t)$ is the envelope, $\varphi(t)$ is the phase of reverberation, and ω_0 is the central frequency.

If the received number of scattered signals at a given time is large, then, in view of the central limit theorem, the reverberation process can be described by a normal distribution in the following form:

$$P(R) = \frac{1}{\sigma\sqrt{2\pi}}\exp\left[-R/2\sigma^2\right], \tag{2}$$

where σ^2 denotes the variance of R. For this signal, the zero mean assumption is valid.

Two main reasons can cause the reverberation process to depart from the Gaussian model: (i) the number of received signals is not large enough, and (ii) some signals predominate over the rest and yield a significant contribution to the process.

In general, for non-Gaussian processes, the probability density function (pdf) of reverberation is approximated by the series

$$\begin{aligned} P(R) =& \frac{1}{\sigma\sqrt{2\pi}}\exp\left[-R/2\sigma^2\right] \times \left[1 + \frac{1}{3!}\frac{\mu_3}{\sigma^3}H_3(R/\sigma)\right. \\ &\left. + \frac{1}{4!}\left(\frac{\mu_4}{\sigma^4} - 3\right) + H_4(R/\sigma) + \cdots\right], \end{aligned} \tag{3}$$

where $H_k(x)$ is a kth-order Hermite polynomial, and μ_i are the central moments of R.

Assuming quasi-harmonic signals (all odd moments are zero), the zero-mean reverberation pdf is then given by

$$P(R) = \frac{1}{\sigma\sqrt{2\pi}}\exp\left[-(R/2\sigma^2)\right] \times \left[1 + \frac{1}{4!}\left(\frac{\mu_4}{\sigma^4} - 3\right) + H_4(R/\sigma) + \cdots\right]. \tag{4}$$

For purpose of later analysis, we define the *quadrature components* of reverberation as follows:

$$R_{\mathrm{c}}(t) = A(t)\cos\varphi(t), \tag{5}$$

$$R_{\mathrm{s}}(t) = A(t)\sin\varphi(t). \tag{6}$$

Then, the reverberation envelope and phase are given by the expressions

$$A(t) = [R_{\mathrm{c}}^2(t) + R_{\mathrm{s}}^2(t)]^{1/2}, \tag{7}$$

$$\varphi(t) = \tan^{-1}(R_{\mathrm{s}}(t)/R_{\mathrm{c}}(t)). \tag{8}$$

When the reverberation is created with a normal distribution of scatterers, it obeys Gaussian-like probability density functions with zero mean and variances σ_s^2 and σ_c^2. The general appearance of the quadrature pdf is mainly controlled by the *coefficient of excess* or *kurtosis*, γ_{e}, that appears in Eqs. (3) and (4) and is defined in the following way [3,4]:

$$\gamma_{\mathrm{e}} = (\frac{\mu_4}{\sigma^4} - 3). \tag{9}$$

This is a non-dimensional quantity that describes the pointedness or the flatness of the reverberation pdf relative to a Gaussian. Later, it is shown that this parameter is particularly useful in relating the seafloor morphology to the general statistical behavior of bottom reverberation.

2.2. RANDOM SURFACE GENERATION

The generation of a random seafloor segment of length L is based on the inverse spectrum technique. It is assumed that the roughness spectrum obeys Gaussian statistics and its spectral density is given by the following expression:

$$W(K) = \tfrac{1}{4}\big(lh^2/(2\sqrt{\pi})\big)e^{-K^2l^2}, \tag{10}$$

where h is the surface rms height, l is the correlation length, and K is the spatial wave number.

From Eq. (10), it is observed that the correlation length is inversely proportional to the standard deviation of the bottom surface, while the rms height is a measure of the roughness power since

$$\int_{-\infty}^{+\infty} W(K)\,\mathrm{d}K = h^2. \tag{11}$$

The discrete roughness representation is defined by a set of N points with spacing Δx, and thus, surface length $L = N\Delta x$. Then, the Fourier transform of the random seafloor can be written as follows [6]:

$$F(K_j) = \begin{cases} \big[2\pi LW(K_j)\big]^{1/2}\big[N(0,1) + iN(0,1)\big]/\sqrt{2}, & j \neq 0, \tfrac{1}{2}N \\ \big[2\pi LW(K_j)\big]^{1/2}N(0,1), & j = 0, \tfrac{1}{2}N, \end{cases} \tag{12}$$

where $K_j = 2\pi j/L$ is the spatial wavenumber for $j \geq 0$, and $N(0,1)$ indicates independent samples taken from a zero mean, unit variance Gaussian distribution. For $j < 0$, we have $F(K_j) = F(K_{-j})^*$.

The surface realization is computed with the inverse Fourier transform of $F(K)$:

$$f(x_n) = \frac{1}{L} \sum_{j=-N/2}^{(N/2)-1} F(K_j) e^{iK_j x_n}, \tag{13}$$

where $x_n = n\Delta x$ and $n = 1, 2, \ldots N$.

Figure 1 shows three surfaces generated by this method. The first two have the same correlation length 5 m, but the average height of the second surface (4 m) is twice the height of the first (2 m). Although the magnitude of the roughness increased, the relation between neighboring points remained the same. On the other hand, the first and the third surfaces are created with the same average height (2 m) but different correlation lengths (first surface $l = 5$, second surface $l = 30$). As a result, the last surface has a much smoother appearance due to a greater value of surface-point correlation (30 m).

Note The rough bottom profile generated with this method is imported into the 2WAYPE input file as a set of discrete points that represent the range and depth coordinates (x_n, fx_n) of the seafloor. The 2WAYPE program connects these points using the stair-step approximation, which means that the actual simulated bottom does not have a smooth appearance as in Fig. 1. Instead, it comprises of a train of step functions with random amplitudes fx_n, see Fig. 2.

2.3. SCENARIOS UNDER INVESTIGATION

The main goal of this work is to relate the statistical behavior of the reverberation signal with morphological features of the rough bottom. These features are modeled via two surface parameters, namely the rms height h and correlation length l.

To investigate this problem, six families of seafloors are generated using two h-values (i.e. 7.5 m, which equals the wavelength of the central frequency, and 30 m), and three l-values (i.e. 5 m, 50 m and 100 m). Each family consists of five random rough surface realizations created with the same set of parameters. The seafloor profile is generated using the MATLAB software package (Annex C). The outcome of this program is manually imported into a standard input 2WAYPE file. Then, the 2WAYPE (VAX Fortran) routine is called to calculate the channel response. The statistical analysis of the reverberation signal is performed in the MATLAB environment.

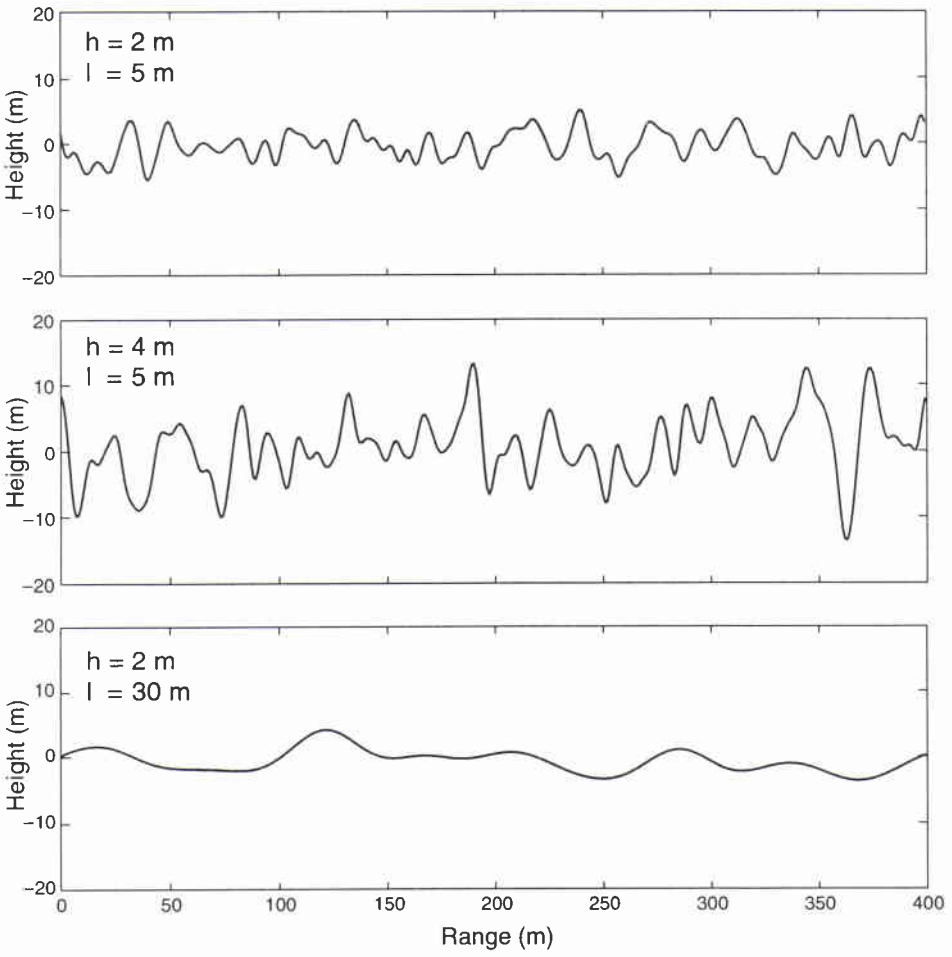

Figure 1 *Random surfaces created with different combinations of average height (h) and correlation length (l).*

2.4. STATISTICAL MEASUREMENTS

The underwater channel frequency response is transformed to a time series using IFFT methods (MATLAB library) [12]. The quadrature components of reverberation correspond to the real and imaginary parts of the time domain channel response. Fig. 3 represents statistical characteristics from a rough segment generated with $h = 7.5$ m and $l = 5$m. Fig. 3a shows the real reverberation time series calculated at the receiver location, while Figs. 3b,c show the histograms of both quadrature components, and Figs. 3d,e show the histograms of the amplitude and phase of reverberation. Three key statistical parameters of this process are given in Table 1.

For a preliminary comparison, Fig. 4 shows the statistical profile for a propagation scenario created with surface height $h = 7.5$ m and much larger correlation $l = 100$ m (in this case the scattering surface is much smoother). The corresponding statistical

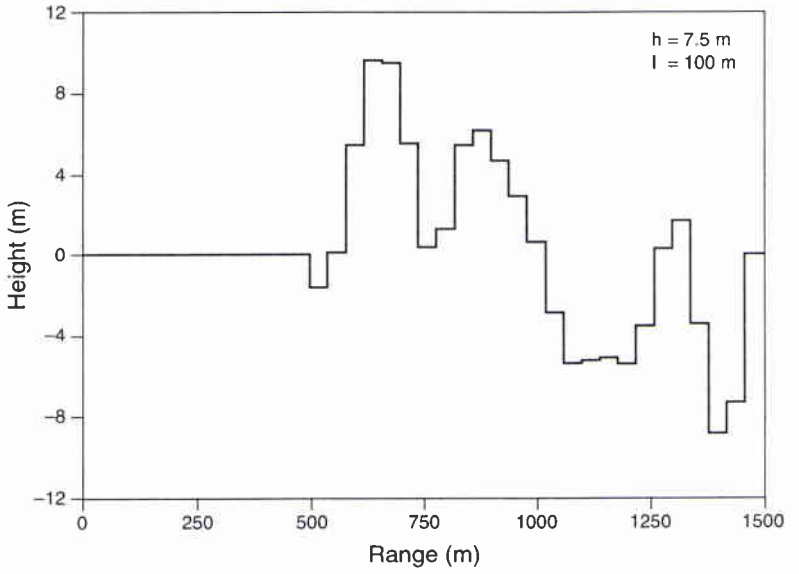

Figure 2 *Stair-step bottom profile as simulated by the* 2WAYPE *program.*

parameters are given in Table 2.

As predicted by the reverberation theory, both processes have zero-mean, symmetric distributions (see Eqs. (3) and (4)). It is also noticeable that their variance is not very sensitive to different values of the surface correlation length. On the contrary, these two scenarios demonstrate a significant difference in the value of kurtosis. Additionally, the fact that $\gamma_e \gg 0$ implies that the pdf's of these processes diverge from the Gaussian model (under the definition of kurtosis given in Eq. (9), Gaussian pdf's have zero kurtosis). A similar behavior is observed for different combinations of h and l, as well as, different random realizations for the same set of parameters. Figures 5–8 correspond to the remaining representatives of the following families of surfaces: (Fig. 5: $h = 7.5$ m, $l = 50$ m), (Fig. 6: $h = 30$ m, $l = 5$ m), (Fig. 7: $h = 30$ m, $l = 50$ m), and (Fig. 8: $h = 7.5$ m, $l = 100$ m). For each combination of h and l, the experiment is repeated five times; each time different random numbers are used in the generation of the seafloor (see Eqs. (12)). The values for the variance and kurtosis for each case are shown in Table 3.

The first column demonstrates a general trend toward higher values of σ^2 when the surface roughness increases. This is an expected result since, the higher the maximum allowed height, the larger the number of intermediate roughness heights, and thus the greater the variance of the backscattered signal. This behavior has a 'spreading' effect on the abscissa of the quadrature histogram. On the contrary, the relationship between the correlation length of the seafloor and the reverberation signal is not so clear. The values of σ^2 are similar for different values of l (see Table 3). Initial results (Tables 1 and 2) point toward the kurtosis as a suitable statistical means to approach this comparison.

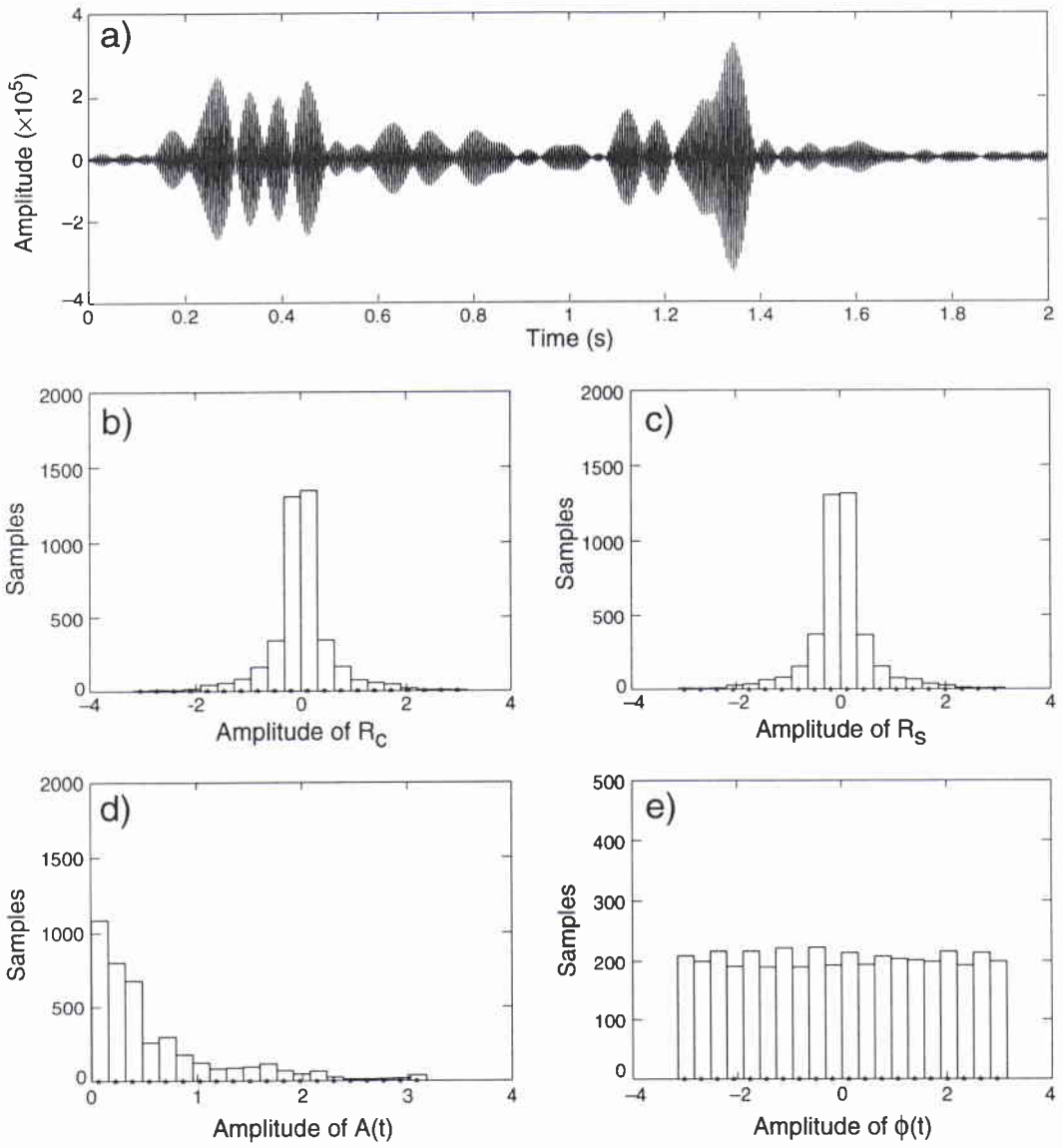

Figure 3 *Statistical characteristics from a rough segment generated with $h = 7.5$ m and $l = 5$ m: (a) reverberation time series; (b),(c) histograms of reverberation quadrature components; (d),(e) histograms of reverberation amplitude and phase*

Table 1 *Statistical parameters corresponding to Fig. 3*

Seafloor rms height $h = 7.5$ m	Correlation length $l = 5$ m	
mean $\mu = 0$	variance $\sigma^2 = 0.3726$	kurtosis $\gamma_e = 4.9951$

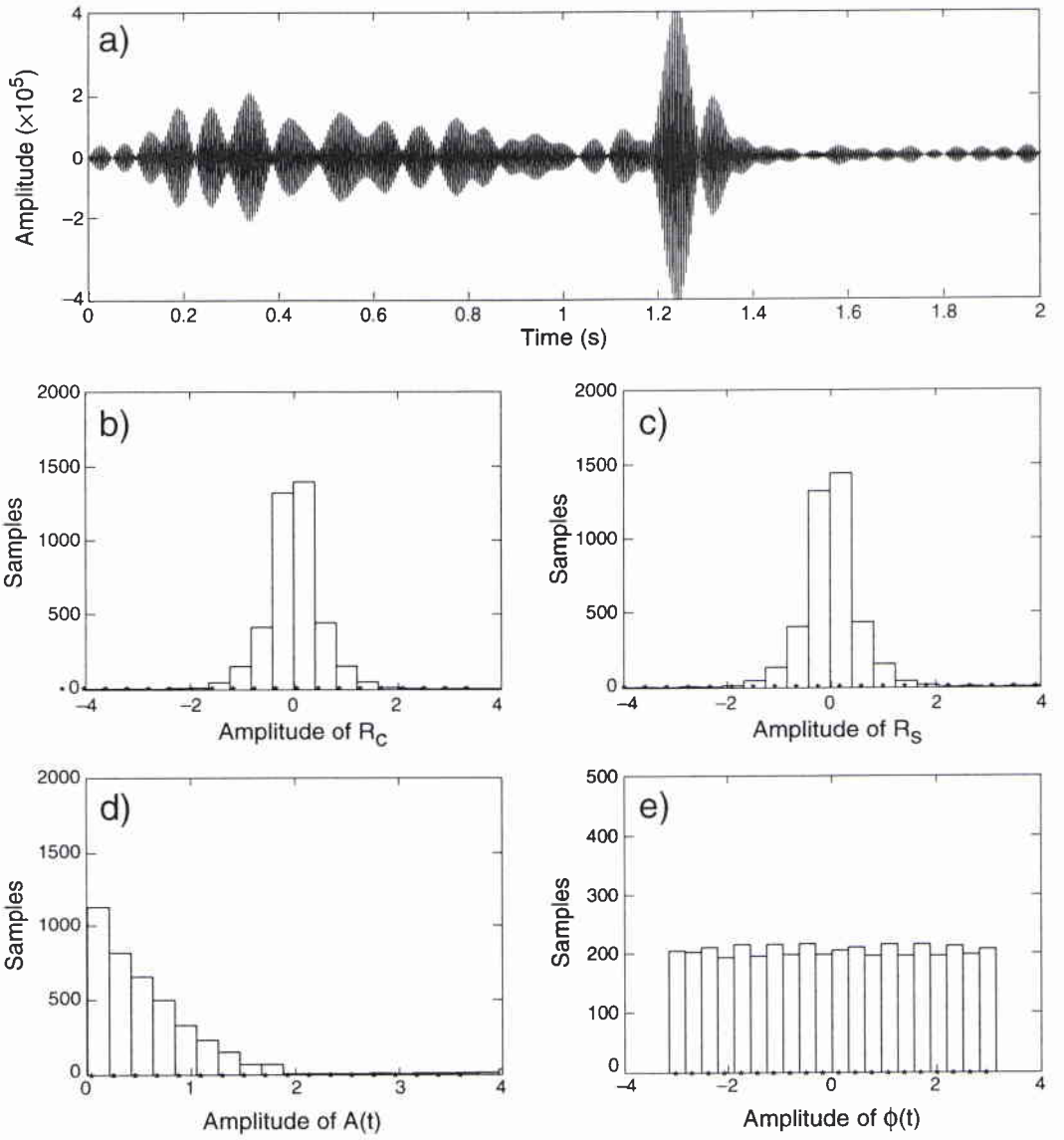

Figure 4 *Statistical characteristics from a rough segment generated with $h = 7.5$ m and $l = 50$ m: (a) reverberation time series; (b),(c) histograms of reverberation quadrature components; (d),(e) histograms of reverberation amplitude and phase*

Table 2 *Statistical parameters corresponding to Fig. 4*

Seafloor rms height $h = 7.5$ m	Correlation length $l = 5$ m	
mean $\mu = 0$	variance $\sigma^2 = 0.4158$	kurtosis $\gamma_e = 9.5351$

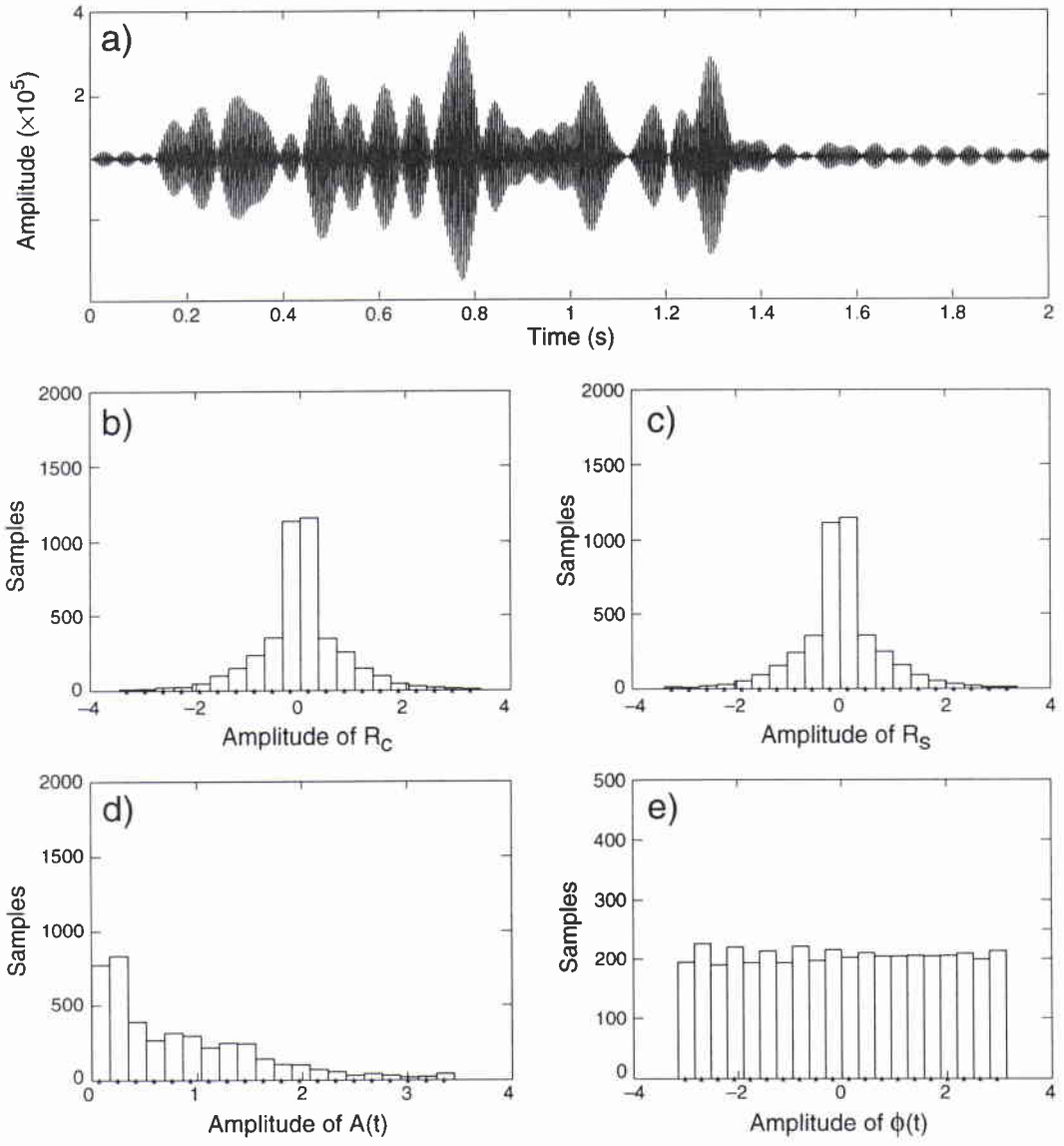

Figure 5 *Statistical characteristics from a rough segment generated with $h = 7.5$ m and $l = 100$ m: (a) reverberation time series; (b),(c) histograms of reverberation quadrature components; (d),(e) histograms of reverberation amplitude and phase*

For a better comparison between the various cases, the average value of kurtosis, i.e. $\langle \gamma_e \rangle$, is calculated from the five simulation experiment performed for each combination of h and l. $\langle \gamma_e \rangle$ is a meaningful parameter to be employed in this comparison for two reasons: (i) the results do not rely on some variation of the random nature of the problem, and (ii) averaging different segments of the same family of surfaces compensates for the small number of points ($N = 25$) used in each segment. This restriction in N is necessary in order to maintain a computationally efficient propagation scenario.

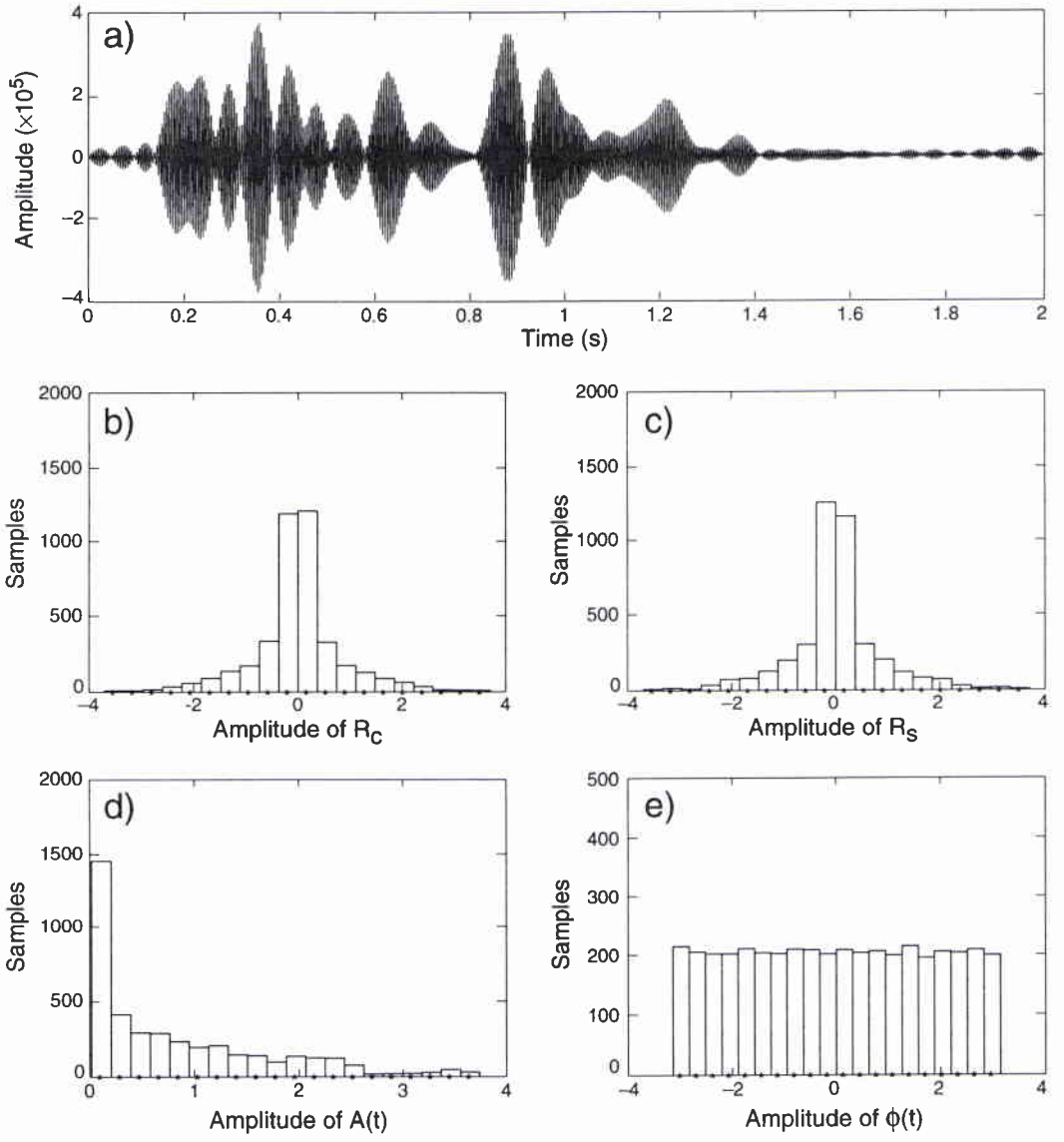

Figure 6 *Statistical characteristics from a rough segment generated with $h = 30$ m and $l = 5$ m: (a) reverberation time series; (b),(c) histograms of reverberation quadrature components; (d),(e) histograms of reverberation amplitude and phase*

Plots of $\langle \gamma_e \rangle$ versus surface rms height appear in Fig. 9. The three plots correspond to rough seafloor correlation lengths of 5 m, 50 m, and 100 m. The solid lines that represent the mean value of γ_e are bounded by two dotted lines that correspond to γ_e plus and minus its standard deviation. Figure 10 shows the comparison between the mean values of γ_e for the three values of correlation length, i.e. $l = 5$, 50, 100 m. From these plots it is apparent that γ_e is proportional to the rough surface correlation length. This is intuitively sensible because for large values of l the seafloor appears to be smooth. This implies that the variability of the received signal are

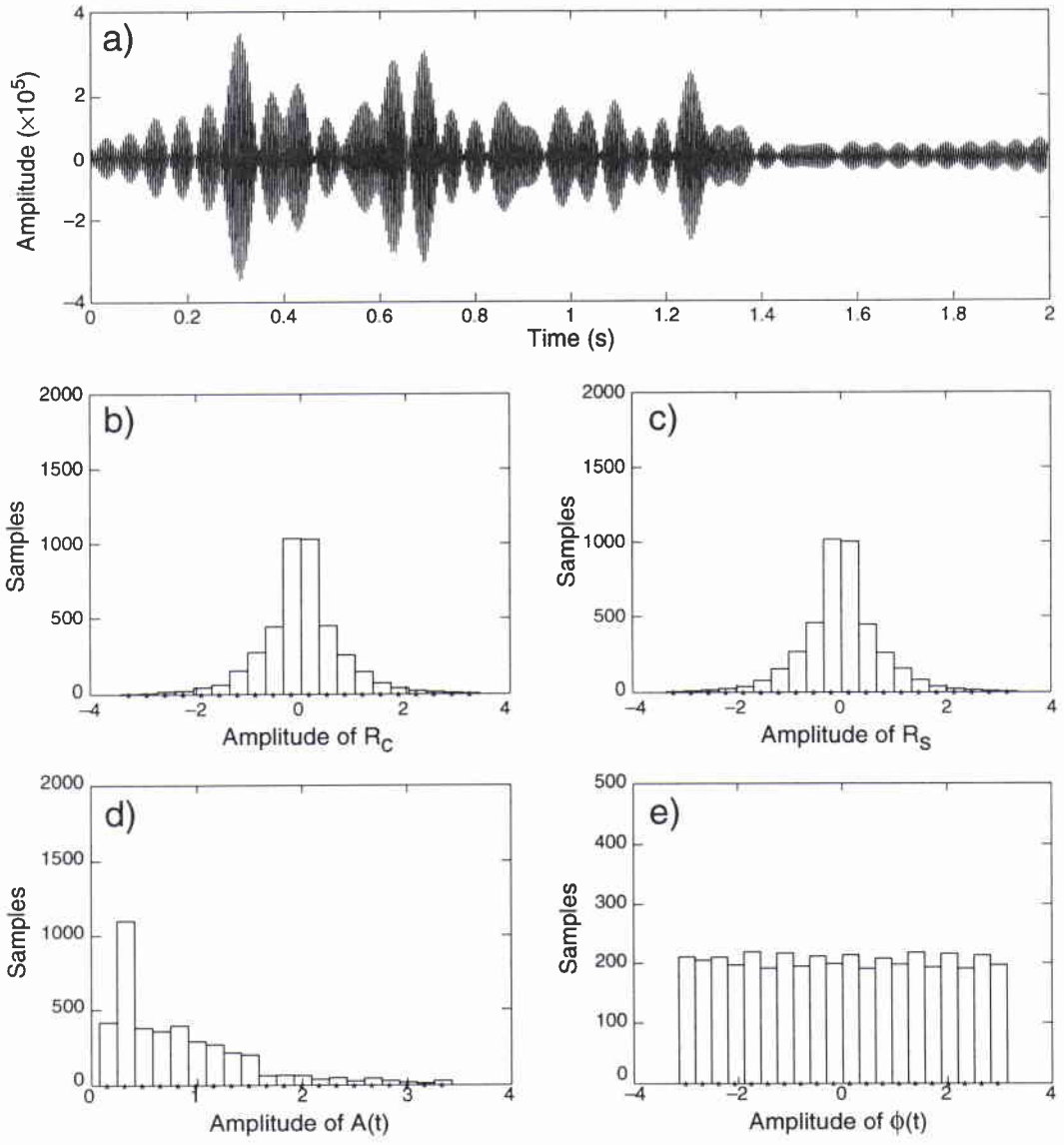

Figure 7 *Statistical characteristics from a rough segment generated with $h = 30$ m and $l = 50$ m: (a) reverberation time series; (b),(c) histograms of reverberation quadrature components; (d),(e) histograms of reverberation amplitude and phase*

small, and thus, the probability density (or histogram) of the reverberation appears to be very peaky. This is an indication of high values of kurtosis γ_e. On the other hand, for small values of the correlation length, the seafloor has a 'noisy' appearance which creates a backscattered signal that incorporates a large number of different amplitudes values. Consequently, the histograms of the quadrature components of reverberation appear flatter, which indicates small values of γ_e.

Another important observation from Fig. 10 is that for either small (5 m) or large

Table 3 *Values for the variance and kurtosis for each case*

Seafloor parameters	Variance σ^2	Kurtosis γ_e
$h = 7.5$ m, $l = 5$ m	0.3556	3.4793
	0.2283	5.6495
	0.3415	2.7565
	0.3040	2.0855
	0.3726	4.9951
$h = 7.5$ m, $l = 50$ m	0.5845	2.6438
	0.3103	3.8143
	0.4355	5.2274
	0.4336	3.5551
	0.3403	1.7951
$h = 7.5$ m, $l = 100$ m	0.2191	6.5336
	0.4661	6.1177
	0.2140	6.8079
	0.2967	3.3226
	0.4158	9.5351
$h = 30$ m, $l = 5$ m	0.5286	2.1250
	0.4999	3.1660
	0.6446	4.2247
	0.7290	2.9974
	0.3440	3.0607
$h = 30$ m, $l = 50$ m	0.5779	2.4951
	0.5456	6.7060
	0.5781	2.4951
	0.6814	6.0707
	0.8903	7.3873
$h = 30$ m, $l = 100$ m	0.6091	8.5127
	0.9564	10.2135
	0.8923	5.1419
	1.0187	2.7907
	0.7098	6.6010

(100 m) values of l, kurtosis does not change significantly with respect to h. This is not a suprising result because the correlation length is the parameter which controls the 'noisiness' of the seafloor while the height acts as a scaling factor of the roughness without changing the spatial relationship of neighbouring points. Finally, for the intermediate value of 50 m, it is observed that the kurtosis increases proportionally to h. This is a transition range of kurtosis values which is probably related to the small number of roughness points that does not allow a full development of the desired surface profile.

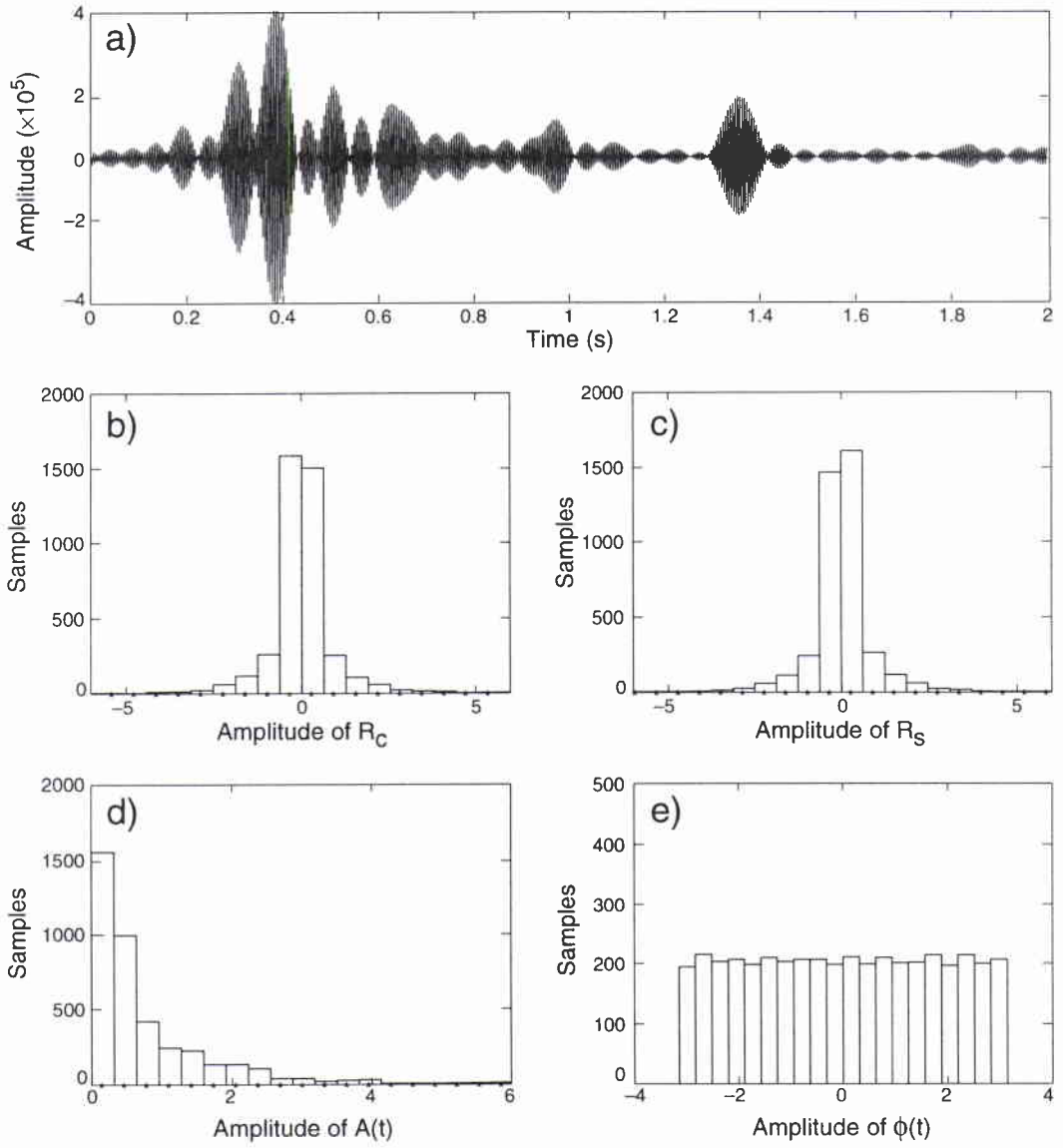

Figure 8 *Statistical characteristics from a rough segment generated with $h = 30$ m and $l = 100$ m: (a) reverberation time series; (b),(c) histograms of reverberation quadrature components; (d),(e) histograms of reverberation amplitude and phase*

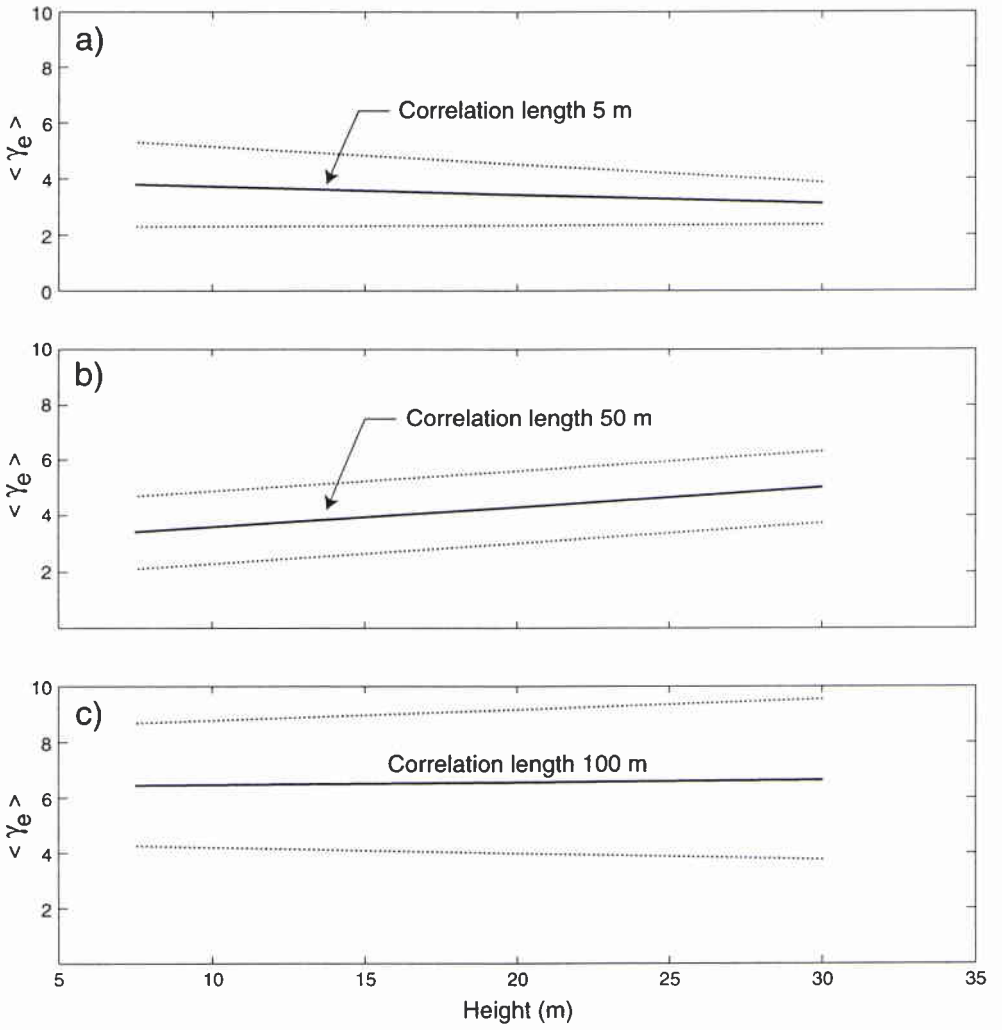

Figure 9 *Average kurtosis (solid lines) vs surface height: (a) $l = 5$ m; (b) $l = 50$ m; (c) $l = 100$ m. (The dotted lines represent the average value of kurtosis plus or minus its standard deviation.)*

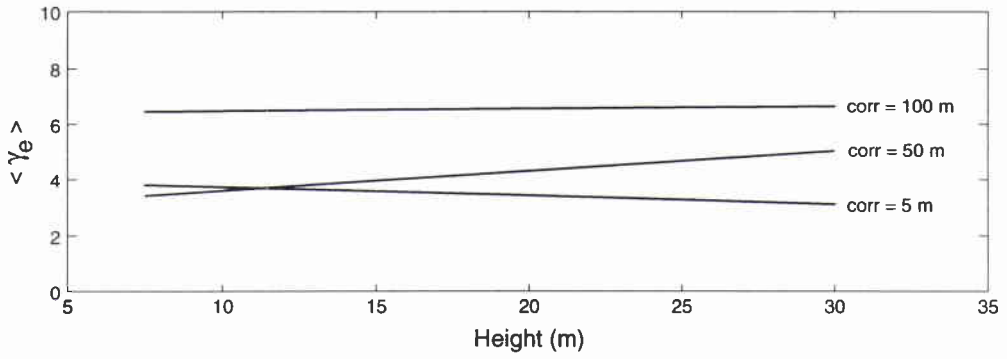

Figure 10 *Comparison between the three average values of kurtosis shown in Fig. 9 corresponding to different surface correlation lengths:* $l = 5\ m$, $l = 50\ m$, *and* $l = 100\ m$.

3

Conclusions and future plans

Computer simulations were used for the statistical analysis of large-scale reverberation from the ocean terrain. A relation between the general seafloor morphology and moments of the received signal time series was established. It was found that the probability density of the quadrature components of reverberation diverge from a Gaussian pdf, since large bottom discontinuities generate strong signal returns that dominate over weaker reponses from smaller bottom features. Also, the variance of reverberation appears to increase proportionally with the surface rms height. This occurs because the higher the maximum allowed roughness, the larger the number of intermediate roughness amplitudes on the seafloor. The above implies that many individual signals with different backscattered responses arrive at the receiver, thus causing the variability of the total reverberation response to increase.

On the contrary, the kurtosis (or coefficient of excess) does not seem to be very sensitive to changes in roughness height. This parameter was found to be closely related to the correlation length of the rough boundary. In particular, reverberation generated from surfaces with smooth appearance (i.e. large value of correlation length) demonstrates higher values of kurtosis relative to cases with a much rougher seafloor. This behaviour is explained by the fact that a very smooth surface causes a uniform scattering of the incident signal, resulting in a narrow pointed pdf. On the other hand, the 'noisy' appearance of a small correlation length surface is responsible for a larger number of similar backscattered signals which gives a flatter appearance to the pdf. Note that, in this case, although the number of individual signals increases, the variance of the pdf remains the same because the average roughness does not change and thus all backscattered signal responses are of the same order.

This work represents only one approach to the general problem of modeling large-scale reverberation from a rough seafloor. Further work in this direction could include correlation and power spectrum analysis, optimization of receiver location, and comparisons between experimental and theoretical probability density functions.

References

[1] Anderson, V.C. Frequency dependence of reverberation in the ocean. *Journal of the Acoustical Society of America*, **41**, 1967: 1467–1474.

[2] Wilson, G.R. A statistical analysis of surface reverberation. *Journal of the Acoustical Society of America*, **74**, 1983: 249–255.

[3] Alexandrou, D., de Moustier, C. and Haralabus, G. Evaluation and verification of bottom acoustic reverberation statistics predicted by the point scattering model. *Journal of the Acoustical Society of America*, **91**, 1992: 1403–1413.

[4] Ol'shevskii V.V. Characteristics of Sea Reverberation. New York, N.Y., Consultants Bureau, 1967. [LCCN 67-025401]

[5] Ol'shevskii V.V. Statistical Methods in Sonar. New York, N.Y., Consultants Bureau, 1978. [ISBN 0-306-10947-6]

[6] Thorsos, E.I. The validity of Kirchhoff approximation for rough surface scattering using a Gaussian roughness spectrum. *Journal of the Acoustical Society of America*, **83**, 1988: 78–92.

[7] Collins, M.D. and Evans, R.B. A two-way parabolic equation for acoustic backscattering in the ocean. *Journal of the Acoustical Society of America*, **91**, 1992: 1357–1368.

[8] Collins, M.D. FEPE user's guide, NORDA TN 365. Stennis Space Center, MS, Naval Ocean Research and Development Activity, 1988. [AD B 128 889]

[9] Collins, M.D. and Werby, M.F. A parabolic equation model for scattering in the ocean. *Journal of the Acoustical Society of America*, *85*, 1989: 1895–1902.

[10] Evans, R.B. COUPLE: a user's manual, NORDA TN 332. Stennis Space Center, MS, Naval Ocean Research and Development Activity, 1986. [AD B 106 858]

[11] Evans, R.B. A coupled mode solution for acoustic propagation in a waveguide with stepwise depth variation of a penetrable bottom. *Journal of the Acoustical Society of America*, **74**, 1983: 188–195.

[12] Anon. 1993. Matlab for VAX/VMS Computers. Natick, MA, The MathWorks Inc., 1991.

[13] Urick, R.J. Principles of Underwater Sound, 3rd edn. New York, N.Y. McGraw-Hill, 1983. [ISBN 0-07-066087-5]

[14] Clay, C.S. and Medwin, H. Acoustical oceanography: Principles and applications. New York, N.Y., Wiley, 1977. [ISBN 0-471-16041-5]

[15] Burdic, W.S. Underwater Acoustic System Analysis. Englewood Cliffs, N.J., Prentice-Hall, 1991. [ISBN 0-13-947607-5]

[16] Tappert, F.D. 1977. The parabolic approximation method. *In*: Keller, J.B. and Papadakis, J.S., *eds.*. Wave Propagation and Underwater Acoustics. New York, N.Y., Springer-Verlag, pp. 224–285. [ISBN 0 387 08527 0]

[17] Jensen, F.B., Kuperman, W.A., Porter, M.B., and Schmidt, H. Computational Ocean Acoustics. Woodbury, N.Y., American Institute of Physics, 1994. [ISBN 1-56396-2098]

Annex A

Wave propagation models: The parabolic equation model

The cornerstone of the 2WAYPE model is the solution of higher-order parabolic equations (PE). This PE method is an alternative technique to the classical approaches for solving sound propagation problems, i.e. normal mode and ray tracing models. A brief discussion and comparison between these three methods illustrates the novelty of the PE technique.

In *normal mode* theory the acoustic waves are described in terms of characteristic functions, each of which is a solution to the wave equation. The pressure field is expressed as the sum of an infinite number of normal modes. To create a numerically feasible solution, only a finite number of these modes are propagated and the rest are considered evanescent. The advantage of this approach is that it gives a formally complete solution which is relatively easy to implement. This is one of the chief reasons for normal mode theory being particularly suited for the complex shallow water environment. Its basic disadvantage is that it is designed for a horizontally-stratified ocean of constant depth. Also, although it is valid for all frequencies, it is particularly useful for low frequencies which can be described with only a few modes [13–15].

The *ray tracing* model is based on the principle of wavefronts along which the solution has constant phase. It is assumed that the acoustic wavelength is very small compared with the distances over which the sound-velocity profile changes considerably. The acoustic paths, similarly to optics, are pictured using ray diagrams (Snell's law). Therefore, one of the advantages of this method is that it provides physical intuition about the propagation of sound in the ocean. Also, this model is not restricted to a horizontally-stratified propagation channel; it can accommodate horizontal variations of the sound-velocity profile, as well as bathymetric variations. The main disadvantages are that it does not take into account diffraction effects, it is restricted only to high frequencies, and the field becomes infinite on caustic surfaces (the envelope surface of a convergence zone) [13–15].

An alternative method that deals with both horizontal changes of sound speed and depth variations is the *parabolic equation* method. This technique is suited for harmonic waves propagating mainly in one direction (e.g. the range direction). Its principle advantage over the methods previously described is that it provides a numerical solution which is considerably easier to be calculated. Using the parabolic equation method, the acoustic pressure along the propagation channel can be solved using marching techniques in one direction. This makes it particularly fitted for solving

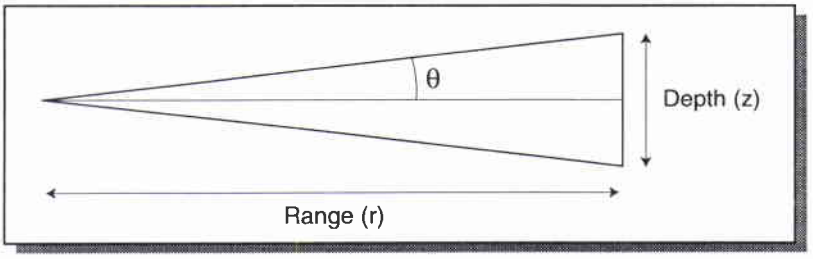

Figure A1 *Geometry for small transmission angle θ.*

complex range-dependent problems. The disadvantage of the method is that it is inaccurate when rays are bending significantly in either the horizontal or the vertical direction. Also its validity is questionable for large bottom discontinuities, such as steep slopes and high steps [16].

The basic idea of the parabolic equation is illustrated in the following example. In a 2-dimensional uniform medium, the expression for the pressure field

$$p = \frac{1}{\sqrt{r^2 + z^2}} \exp\Big(ik\Big[\sqrt{r^2 + z^2}\Big]\Big) \tag{A1}$$

satisfies the Helmholtz equation in cylindrical coordinates:

$$\frac{\partial^2 p}{\partial r^2} + \frac{1}{r}\frac{\partial p}{\partial r} \frac{\partial^2 p}{\partial z^2} + k^2 n^2 p = 0, \tag{A2}$$

where $k = \omega/c_0$ is the wavenumber, $n(r, z) = c_0/c(r, z)$ is the index of refraction, and r, z denote range and depth respectively.

This is a boundary value problem that has to be solved simultaneously for all values of r. In contrast, the parabolic equation method transforms this problem to an initial value case where the solution can be calculated step-by-step along the r-axis.

One possible way to accomplish this is by using the Taylor approximation,

$$\sqrt{1 + x} \approx 1 + \tfrac{1}{2}x, \tag{A3}$$

to simplify the exponential term in (A1) as

$$\sqrt{r^2 + z^2} = r\sqrt{1 + z^2/r^2} \approx r + \tfrac{1}{2}(z^2/r), \tag{A4}$$

provided that the depth is small relative to the range (small angle θ), i.e. $z \ll r \Leftrightarrow z/r \ll 1$ (Fig. A1).

Then, Eq. (A1) can be rewritten as

$$p = \frac{1}{r}\exp\Big(ik\Big[r + \frac{1}{2}\Big(\frac{z^2}{r_2}\Big)\Big]\Big), \tag{A5}$$

or

$$p = \Psi(z,r)\frac{1}{\sqrt{r}}\exp(ikr), \tag{A6}$$

where

$$\Psi(z,r) = \frac{1}{\sqrt{r}}\exp\Big(ik\frac{1}{2}\Big(\frac{z^2}{r}\Big)\Big). \tag{A7}$$

It can be easily shown that Eq. (A5) satisfies the parabolic equation

$$\frac{1}{2k}\frac{\partial^2\Psi}{\partial z^2} + i\frac{\partial\Psi}{\partial r} = 0. \tag{A8}$$

This formula does not include second derivatives with respect to r, and so, it can be solved by a marching method in the range direction. It should be emphasized that a good approximation of the expression $\sqrt{1+x}$ is of paramount importance for an accurate solution. The Taylor approximation which is used in this example is only one of many techniques. Two alternative techniques are described below.

A. The rational-polynomial approximation

$$\sqrt{1+x} \approx \frac{a_0 + a_1 x}{b_0 + b_1 x}, \tag{A9}$$

e.g.

$$\sqrt{1+x} \approx 1 + 0.5x \qquad \text{(Tappert)}, \tag{A10}$$

$$\sqrt{1+x} \approx \frac{1 + 0.75x}{1 + 0.25x} \qquad \text{(Claerbout)}, \tag{A11}$$

$$\sqrt{1+x} \approx \frac{0.99987 + 0.79624x}{1 + 0.30102x} \qquad \text{(Greene)}. \tag{A12}$$

Different approximations are aimed at minimizing phase errors which increase proportionally to transmission angles. So, although Eqs. (A11) and (A12) are very similar, the latter is preferable because it produces a much smaller phase error [17].

B. The rational-linear approximation (Padé series) [16],[17]

$$\sqrt{1+x} \approx 1 + \sum_{j=1}^{m} 1 + \frac{a_{j,m}x}{b_{j,m}x} + \mathrm{O}(x^{2m+1}), \tag{A13}$$

where the Padé coefficients are defined as follows

$$a_{j,m} = \frac{2}{2m+1}\sin^2\Big(\frac{j\pi}{2m+1}\Big), \tag{A14}$$

$$b_{j,m} = \cos^2\Big(\frac{j\pi}{2m+1}\Big), \tag{A15}$$

e.g. for one- and two-term Padé approximations

$$\sqrt{1+x} \approx 1 + \frac{0.50x}{1+0.25x} \qquad \text{(one-term)}, \tag{A16}$$

$$\sqrt{1+x} \approx 1 + \frac{0.13820x}{1+0.65451x} + \frac{0.36180x}{1+0.09549x} \qquad \text{(two-term)}. \tag{A17}$$

Currently, the Padé series is the optimal choice in terms of highest accuracy in the propagation direction.

Annex B

The 2WAYPE simulation model

2WAYPE is a Fortran program which computes the forward and the backscattered complex acoustic field relying on the PE method with Padé series approximation. The code models only *line sources* and it assumes *single scattering* from the channel boundaries. In the acoustic channel, range-dependent regions are divided into sequences of smaller, range-independent segments; the propagating sound is approximated by sequentially coupling energy in adjacent range independent bottom areas. At the vertical interface between regions, necessary conditions for continuity of pressure and the normal component of velocity must be satisfied [7].

Example 1 A typical propagation scenario where 2WAYPE is particularly suited is the stairstep ocean bottom shown in Fig. B1 (example B in [7]). The depth is considered constant at 200 m up to 3 km and 100 m between 7 and 10 km. The sound speed is 1500 m/s in the water column and 1700 m/s in the sediment. The density of the homogeneous floor is 1.5 g/cm^3 and the attenuation coefficient is 0.5 dB/λ. A *line* source is situated at 100 m depth and the receiver is placed at 95 m. The frequency of the acoustic signal is 25 Hz. The transmitted and backscattered fields are shown in Fig. B2; a contour plot of the backscattered field appears in Fig. B3.

B.1. UNSTABLE SOLUTIONS

Although the parabolic equation method is an efficient technique for calculating acoustic energy in a range-dependent environment, *its region of validity is not well defined*. As demonstrated here, the model does not always converge to a meaningful solution. Especially at high frequencies, the method is considered suspect for large discontinuities. To demonstrate this point, we consider an ocean-step example similar to the one shown in Fig. B1. Here, the bottom depth is 500 m up to 7 km range, and 250 m between 7 and 10 km. The important change from the referenced problem is that the frequency is increased from 25 Hz to 100 Hz. For this setup, 2WAYPE does not produce a sensible result. As shown in Fig. B4, there is a sharp discontinuity in the acoustic field exactly where the bottom-step is located. That type of problem can be overcome – with some loss of accuracy – by splitting large bottom steps into smaller ones (private communication with Mike Collins). Nevertheless, the present counter example indicates that further work is necessary in comparing the results from 2WAYPE with solutions derived from well tested programs, such as COUPLE. Finally, it should be noted that for the reverberation analysis, small (relative to the wavelength) bottom discontinuities are simulated in order to avoid similar unstable solutions.

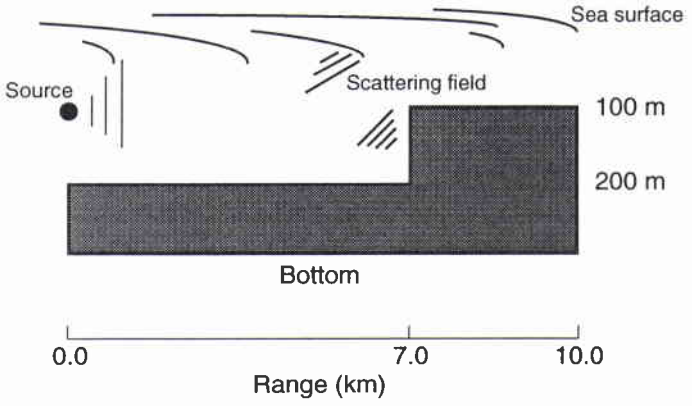

Figure B1 *Simulation geometry with stair-step bottom discontinuity. (Example 1).*

B.2. POINT SOURCE GEOMETRY (CYLINDRICAL SPREADING)

As mentioned before, the 2WAYPE program simulates a line source environment, and thus, only plane waves are allowed to backpropagate at the source. Here we consider a 2-D axisymmetric environment where the scattered field from all azimuthal angles are 'focused' onto the vertical axis located at the origin. To simulate such a point source geometry, the original 2WAYPE code is changed, so that the outcome of the program includes the cylindrical spreading loss. This correction was made by modifying the dB level of the pressure field by an amount that corresponds to the enhancement (or weakening) of the acoustic field due to energy distribution over smaller (or larger) cylindrical surfaces. In particular, assuming that the propagation channel is confined between two parallel planes a distance h apart, the power crossing the cylindrical surfaces at r_1 and r_2 is given by

$$P = 2\pi r_1 h I_1 = 2\pi r_2 h I_2, \tag{B1}$$

where I is the acoustic intensity. Then, the transmission loss between r_1 and r_2 is defined as

$$TL = 10 \log \frac{I_1}{I_2} = 10 \log \frac{r_2}{r_1}. \tag{B2}$$

It should be noted that as $r_1 \to 0$, the transmission loss goes to infinity, $TL \to \infty$, which is an unrealistic focusing situation at the source location (Fig. B5).

Figure B6 shows the backscattered field computed by the 2WAYPE code for both line and point source geometries. The point source simulation is compared with the solution from the COUPLE program (courtesy of F.B. Jensen) which incorporates point source transmission. It is found that the two results are similar, but the computational time of 2WAYPE is considerably less than that of the COUPLE program.

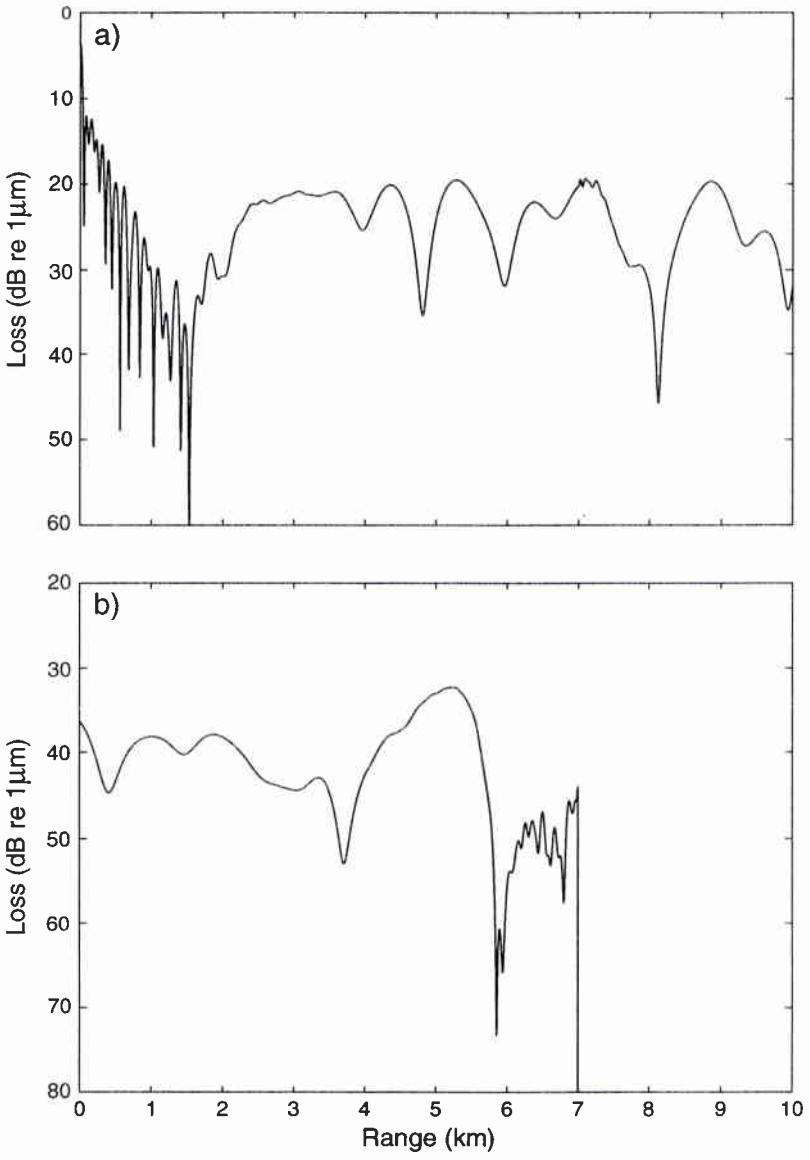

Figure B2 *Transmission loss for (a) the outgoing and (b) the backscattered fields. (Example 1, code:* 2WAYPE*, geometry: Fig. B1).*

B.3. BROADBAND SIGNAL – FOURIER SYNTHESIS

The original 2WAYPE program allows only single-frequency signals to be transmitted. This code was modified (by I. Kirsteins) using Fourier decomposition to accommodate broadband signals. In the new version, the user specifies the minimum (F_{min}) and the maximum (F_{max}) frequencies of the spectrum, the sampling frequency (F_{s}), and the number of Fourier points (N_{F}). The code propagates independent frequencies between F_{min} and F_{max} with increment $F_{\text{s}}/N_{\text{F}}$. The final channel response is the summation of all the individual acoustic pressure fields. The code

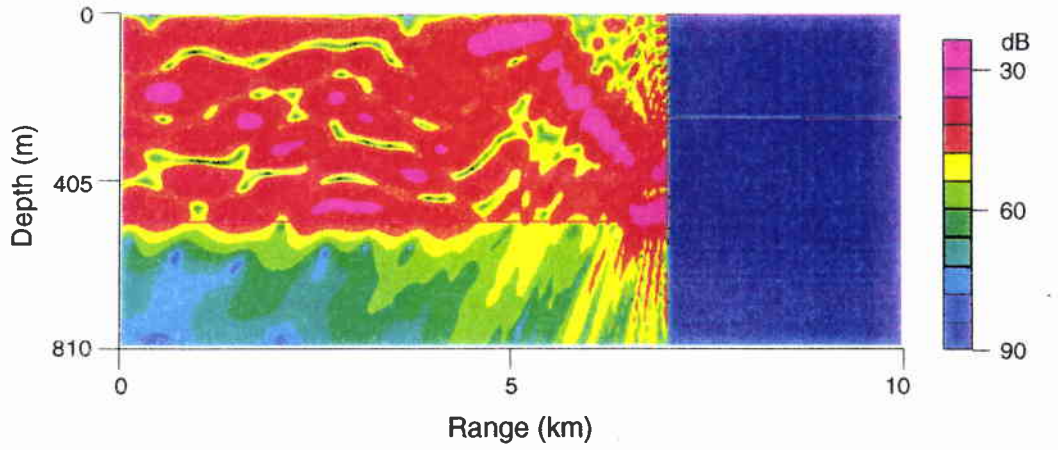

Figure B3 *Transmission loss for the backscattered field (Example 1, code:* 2WAYPE, *geometry: Fig. B1, frequency 25 Hz).*

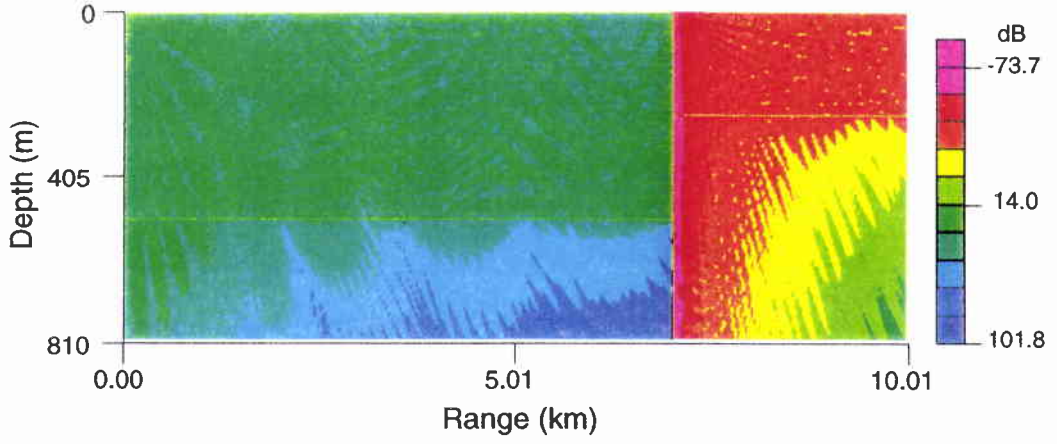

Figure B4 *Transmission loss for the outgoing field (unstable solution example, frequency 100 Hz).*

uses complex notation for the transmitted signals $\left(\cos\omega t = (e^{i\omega x} + e^{-i\omega x})/2\right.$; therefore, for computational efficiency, only half (e.g. negative $e^{-i\omega x}$) of the frequencies are propagated through the medium. Consequently, the outcome of the underwater channel is the complex reverberation envelope $(R_c(t) + iR_s(t))$, with a real part that corresponds to the actual signal response.

For the present analysis of large-scale reverberation, a broadband signal with central frequency $F_c = 200$ Hz and bandwidth BW $= 20$ Hz is used. The minimum and maximum frequencies are $F_{min} = 190$ Hz and $F_{max} = 210$ Hz respectively. The sampling frequency is $F_s = 2048$ samples/s and the number of Fourier points is $N_F = 4096$ (large enough to avoid aliasing affects).The source and the receiver are placed at the same location: 50 m in depth and 0 m in range. The sound speed

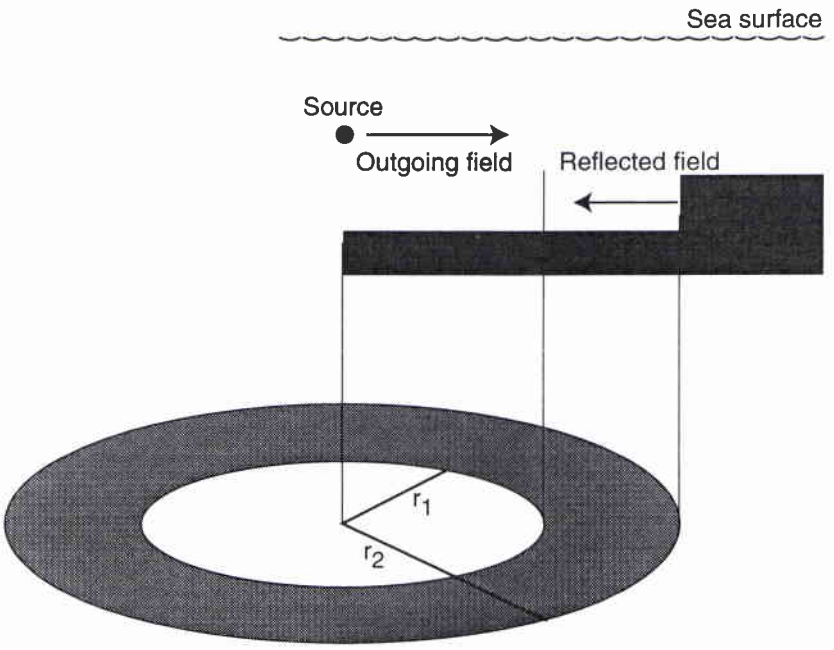

Figure B5 *Cylindrical spreading geometry.*

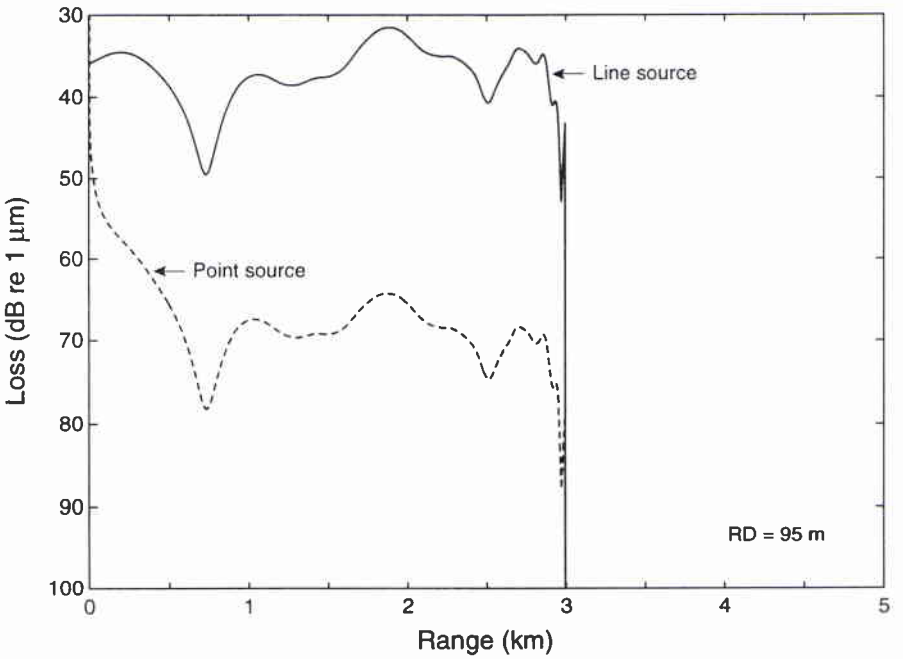

Figure B6 *Line versus point source transmission loss estimation.*

is 1500 m/s in the water and 1600 m/s in the sediment. The seafloor terrain has an attenuation factor of 0.5 dB/λ and density $\rho = 1.5$ g/cm^3. For the first 500 m, the ocean depth is constant at 400 m. The rough seafloor segment spans between 500 and 1500 m in range, and is generated with $N = 25$ discrete points, with 40 m spacing between points.

Annex C

Random surface generation

```
% Georgios Haralabus
% Arpil, 1995

% GAUSSIAN SURFACE SPECTRUM
% [Ref: E.I.Thorsos, JASA 83(1), Jan.1988]

% Control parameters: rms height
%                     correlation length

clear;
clg;

N=input('Enter number of surface points: ');
Dx=input('Enter spacing between points (m): ');

hrms=input('Enter surface rms height (m): ');
cl=input('Enter surface correlation length (m): ');

RB=input('Enter range of first surface point (m): ');
ZB=input('Enter depth of first surface point (m): ');


L=N*Dx      % surface length in meters

% The  rand('normal') was initially used in this code.
% Now this routine is obsolete and it will be eliminated
% in future versions  Instead, use randn().


r=randn(1,2*N);
n=-N/2:N/2-1;

K=(2*pi/L).*n;
WK=(cl*hrms^2/2*sqrt(pi))*exp(-K.^2.*(cl^2/4));

for i=1:N,
        if (n(i)==-N/2 | n(i)==0 | n(i)==N/2-1)
                FK(i)=sqrt(2 * pi * L * WK(i)) * r(2*i);
        elseif (i<N/2)
                FK(i)=sqrt(2 * pi * L * WK(i)) * (r(2*i)+j*r(2*i+1))/sqrt(2.0);
        else
                FK(i)=sqrt(2 * pi * L * WK(i)) * (r(2*i)-j*r(2*i+1))/sqrt(2.0);

        end
end

for i=1:N;
           Xn(i)=(i-1)*Dx;
           fXn(i)=(1/L)*sum(FK.*exp(j*Xn(i)*K) );
end

plot(RB+Xn,real(fXn));
title('Rough bottom segment');
bottom=[RB+Xn;ZB+real(fXn)]';
save bottom.mat bottom /ascii;
```

Report no. changed (Mar 2006): SM-289-UU

Security Classification		Project No.
NATO UNCLASSIFIED		02
Document Serial No.	**Date of Issue**	**Total Pages**
SM-289	July 1995	35 pp.

Author(s)

G. Haralabus

Title

Statistical characteristics of large-scale bottom reverberation

Abstract

Simulation results from a statistical characterization of large-scale bottom reverberation from broad-band signals are presented. The seafloor profile is parametrized via the surface root-mean-square height and correlation length. A connection between these two parameters and the statistical moments of the backscattered signal is established. It is shown that the variance of reverberation increases proportionally to the seafloor root-mean-square height. On the contrary, the kurtosis (or coefficient of excess) of reverberation appears to be independent of changes in roughness height and related to the terrain's smoothness. In particular, it is shown that kurtosis variations are proportional to changes in the seafloor correlation length.

Keywords

bottom reverberation, parabolic equation, scattering

Issuing Organization

North Atlantic Treaty Organization
SACLANT Undersea Research Centre
Viale San Bartolomeo 400, 19138 La Spezia, Italy

[From N. America: SACLANTCEN CMR-426 (New York) APO AE 09613]

tel: +39-187-540.111
fax: +39-187-524.600

e-mail: library@saclantc.nato.int

Initial Distribution for SM-289

SCNR for SACLANTCEN	
SCNR Belgium	1
SCNR Canada	1
SCNR Denmark	1
SCNR Germany	1
SCNR Greece	1
SCNR Italy	1
SCNR Netherlands	1
SCNR Norway	1
SCNR Portugal	1
SCNR Spain	1
SCNR Turkey	1
SCNR UK	1
SCNR US	2
French Delegate	1
SECGEN Rep. SCNR	1
NAMILCOM Rep. SCNR	1

National Liaison Officers	
NLO Belgium	1
NLO Canada	1
NLO Denmark	1
NLO Germany	1
NLO Italy	1
NLO Netherlands	1
NLO UK	3
NLO US	4

Total external distribution	30
SACLANTCEN Library	20
Total number of copies	50